

P2Y₁ receptor activation by photolysis of caged ATP enhances neuronal network activity in the developing olfactory bulb

Timo Fischer · Natalie Rotermund · Christian Lohr · Daniela Hirnet

Received: 28 September 2011 / Accepted: 29 November 2011 / Published online: 22 December 2011
© Springer Science+Business Media B.V. 2011

Abstract It has recently been shown that adenosine-5'-triphosphate (ATP) is released together with glutamate from sensory axons in the olfactory bulb, where it stimulates calcium signaling in glial cells, while responses in identified neurons to ATP have not been recorded in the olfactory bulb yet. We used photolysis of caged ATP to elicit a rapid rise in ATP and measured whole-cell current responses in mitral cells, the output neurons of the olfactory bulb, in acute mouse brain slices. Wide-field photolysis of caged ATP evoked an increase in synaptic inputs in mitral cells, indicating an ATP-dependent increase in network activity. The increase in synaptic activity was accompanied by calcium transients in the dendritic tuft of the mitral cell, as measured by confocal calcium imaging. The stimulating effect of ATP on the network activity could be mimicked by photo release of caged adenosine 5'-diphosphate, and was inhibited by the P2Y₁ receptor antagonist MRS 2179. Local photolysis of caged ATP in the glomerulus innervated by the dendritic tuft of the recorded mitral cell elicited currents similar to those evoked by wide-field illumination. The results indicate that activation of P2Y₁ receptors in the glomerulus can stimulate network activity in the olfactory bulb.

Keywords Mitral cell · Calcium imaging · Synaptic integration · Olfactory glomerulus · Patch clamp

Timo Fischer and Natalie Rotermund contributed equally to the study.

Electronic supplementary material The online version of this article (doi:10.1007/s11302-011-9286-z) contains supplementary material, which is available to authorized users.

T. Fischer · N. Rotermund · C. Lohr · D. Hirnet (✉)
Division of Neurophysiology, Biocenter Grindel,
University of Hamburg,
Martin-Luther-King-Pl. 3,
20146 Hamburg, Germany
e-mail: daniela.hirnet@uni-hamburg.de

Introduction

Adenosine-5'-triphosphate (ATP) not only is an ubiquitous energy currency in all cells, but also an intercellular messenger involved in controlling a variety of physiological processes such as blood pressure, platelet aggregation, and immune responses [1]. In addition, ATP is released as a neurotransmitter in the peripheral and central nervous system [2–4]. ATP acts on two classes of receptors, referred to as P2X and P2Y receptors. P2X receptors are ligand-gated nonselective cation channels, whereas P2Y receptors belong to the large family of G protein-coupled receptors. P1 receptors, another class of G protein-coupled receptors, are activated by adenosine that results from the enzymatic breakdown of ATP by ectonucleotidases [5].

P1 receptors as well as P2X and P2Y receptors are widely expressed in the vertebrate brain, where they shape neuronal activity in multiple modes [6]. P2X receptors are involved in fast synaptic transmission, e.g., in the medial habenula, the hippocampus, and the cerebral cortex [7–9]. P1 and P2Y receptors mediate synaptic plasticity by interaction with ion channels and receptors in many (if not all) brain regions such as the hippocampus, the cerebellum, the striatum and cerebral cortex [10–12]. In the mouse olfactory bulb, evidence for functional expression of purinoceptors was published only recently (reviewed in [13]). Axons of olfactory receptor neurons which connect the olfactory epithelium with second order neurons in the olfactory bulb (mitral/ tufted cells) release ATP together with glutamate [14]. ATP activates P2Y₁ receptors of glial cells ensheathing bundles of sensory axons which results in glial calcium signaling [15]. In addition, axons of olfactory receptor neurons release ATP at synaptic terminals where it stimulates calcium signaling in astrocytes via P2Y₁ receptors and, after degradation to adenosine, P1 receptors of the A_{2A} subtype

[16]. Calcium signaling in olfactory bulb neurons, however, could not be recorded upon application of ATP in these studies, although histological data imply the expression of P2X receptors in mitral cells, granule cells, periglomerular cells, and sensory axons themselves in the olfactory bulb [17–20]. This discrepancy could be explained by technical inadequateness of the calcium imaging studies to record purinergic responses in neurons. Firstly, bulk loading of calcium indicators such as Fluo-4 preferentially loads glial cells and interneurons, whereas mitral cells were not loaded and hence were not recorded in the imaging studies [16]. Secondly, the slowly rising ATP concentration during bath application could cause desensitization of P2X receptors at relatively low concentrations and hence before a sufficient number of receptors is activated to elicit a significant calcium increase. To circumvent these problems, we used photolysis of caged purines to evoke a rapid rise in extracellular purine concentration and measured synaptic currents in mitral cells as a monitor of network activity in olfactory bulb slices. Photolysis of caged ATP and caged adenosine 5'-diphosphate (ADP) evoked an increase in glutamatergic and GABAergic synaptic currents via P2Y₁ receptors, indicating that P2Y₁ receptors increase network activity in the olfactory bulb, whereas we did not find evidence for P2X receptor-mediated signaling.

Materials and methods

Slice preparation

Olfactory bulb slices were prepared from postnatal NMRI mice (P3–P13) as described before [21]. Mice were anesthetized with isoflurane and decapitated. Olfactory bulbs were quickly transferred into a chilled calcium-reduced (0.5 mM Ca²⁺) artificial cerebrospinal fluid (ACSF, see below). 200 μm thick horizontal slices of the bulbs were cut using a vibratome (Leica VT1200S, Bensheim, Germany). Brain slices were stored in ACSF for 30 min at 30°C and 15 min at room temperature before starting experiments. ACSF was continuously gassed with carbogen (95% O₂/5% CO₂; buffered to pH 7.4 with CO₂/bicarbonate).

Solutions

The standard ACSF for acute brain slices contained (in mM): NaCl 125, KCl 2.5, CaCl₂ 2, MgCl₂ 1, D-glucose 25, NaHCO₃ 26, NaH₂PO₄ 1.25, gassed during the entire experiment with carbogen to adjust the pH to 7.4. In calcium-reduced ACSF (0.5 mM), 1.5 mM CaCl₂ was replaced by 1.5 mM MgCl₂. The pipette solution for voltage-clamp experiments contained (in millimolar): CsCl 120, 4-AP 5, EGTA 1, HEPES 10, TEA-Cl 20, Na-glutamate 10, MgCl₂ 2, CaCl₂ 0.5, Na₂ATP 2, NaGTP 0.5. The pipette solution for

current clamp experiments contained (in millimolar): KCl 110, NaCl 10, EDTA 11, HEPES 10, MgCl₂ 1, CaCl₂ 0.5, Mg-ATP 15, Na-GTP 0.5, and phosphocreatine 15. 50 μM Alexa 594 hydrazide (Invitrogen) were added to the pipette solution to visualize the cells.

Caged ATP (adenosine 5'-triphosphate-P3-1-(2-nitrophenyl)ethyl ester; NPE-ATP) was obtained from Merck (Darmstadt, Germany), caged ADP (adenosine 5'-diphosphate-P2-1-(2-nitrophenyl)ethyl ester; NPE-ADP) from MoBiTec (Goettingen, Germany). MRS 2179 (2'-deoxy-N6-methyladenosine 3',5'-bisphosphate tetrasodium salt) was obtained from Tocris (Bristol, UK). D-2-amino-5-phosphonopentanoic acid (D-AP5), 2,3-dioxo-6-nitro-1,2,3,4-tetrahydrobenzo[f]quinoxaline-7-sulfonamide (NBQX), gabazine (2-(3-carboxypropyl)-3-amino-6-(4-methoxyphenyl)pyridazinium bromide), and tetrodotoxin (TTX) were obtained from Ascent Scientific (Weston-Super-Mare, UK). All substances were stored as stock solutions according to the manufacturers' description.

Patch-clamp recordings

Olfactory bulb slices were transferred into a recording chamber (volume ~1.5 ml). Slices were continuously superfused with ACSF, if not stated otherwise. Experiments were performed at room temperature.

Pipettes were pulled from glass capillaries (GC150F-10, Harvard Apparatus, Holliston, MA, USA) on a horizontal puller (P-97, Sutter Instruments, Novato, CA, USA). The resistance of the pipettes when filled with pipette solution was 2–3 MΩ. The whole-cell configuration was established and the command potential was set to -70 mV. Synaptic currents were either recorded using an EPC9 amplifier with Pulse software (HEKA, Lambrecht, Germany) or a Multiclamp 700B amplifier with pClamp 10 software (Molecular Devices, Sunnyvale, CA, USA). Currents were digitized at 10 kHz and Bessel filtered at 2 kHz. In current clamp experiments, the current was set to zero, and post-synaptic potentials were recorded.

Application of ATP and ADP was achieved by photolysis of caged ATP and caged ADP, respectively. Therefore, the perfusion system was stopped and the caged compounds were added to the bath with a micropipette. Caged compounds were allowed to diffuse within the bath for 6 min, after which photolysis of caged ATP or caged ADP was performed (the perfusion still stopped). Wide-field photolysis of caged compounds was achieved by opening the shutter of a 50 mW mercury lamp for 3 s. Most experiments were performed using a Leica microscope (DM LFS), experiments in which membrane current and calcium signaling were recorded simultaneously were performed with a Nikon microscope (FN1). Local photolysis of caged ATP was achieved by illumination of a small field of view (approximately 30×30 μm) with a

405-nm laser for 3 s. Drugs were applied with the perfusion system for 5–10 min, after which the perfusion system was stopped and caged ATP or caged ADP were added to the bath (including the drug) using a micropipette. Photolysis was performed after 6 min. Control experiments and experiments using drugs were performed on different cells, because patch-clamp recordings often did not persist long enough to perform a control experiment in advance of an experiment with drugs on the same cell. However, control experiments were performed on brain slices from the same animals used for experiments with drugs, and hence the recordings employed as control ($n=11$) were gathered throughout the entire period of the project to verify comparable conditions between individual experiments.

Confocal calcium imaging

For calcium imaging in astrocytes, we incubated brain slices with 2 μM Fluo-4 AM (Invitrogen) in standard ACSF for 20–40 min at room temperature [22]. For calcium imaging in mitral cell dendrites, 50 μM Fluo-8 (AAT Bioquest, Sunnyvale, CA, USA) was included in the pipette solution, and EGTA was omitted. Ten to 15 min after establishing the whole-cell configuration, the Fluo-8-filled dendritic tuft of the mitral cell became visible in the glomerular layer. Calcium-dependent changes in Fluo-4 and Fluo-8 fluorescence, respectively, were recorded using a confocal microscope (eC1, Nikon, Düsseldorf, Germany). Fluo-4 and Fluo-8 were excited at 488 nm, and the fluorescence was collected through a 500-nm longpass filter.

Data analysis and statistics

Patch-clamp recordings were analyzed using Mini Analysis (Synaptosoft, Fort Lee, NJ, USA), ClampFit (Molecular Devices) and OriginPro (Northampton, MA, USA). The increase in synaptic activity was either analyzed as the change in the number of synaptic events per 3 s, or as the integral of the current trace, i.e., the area enclosed by the current trace and the baseline (with the resting current as baseline, Supplementary figure 1). Changes in the cytosolic calcium concentration in astrocytes and in the dendritic tufts were reflected as changes in Fluo-4 and Fluo-8 fluorescence, respectively. The fluorescence was normalized to the resting fluorescence (set to 100%) for comparability. Changes in fluorescence are given as ΔF in % of the resting fluorescence. All values are means \pm standard error of the mean with n representing the number of analyzed cells. Data from at least three individual animals were used for each data set. We did not observe major differences in the responsiveness towards ATP between individuals. Significances of statistical differences were calculated using Student's t test. Means were defined as statistically different at an error probability $p < 0.05$.

Results

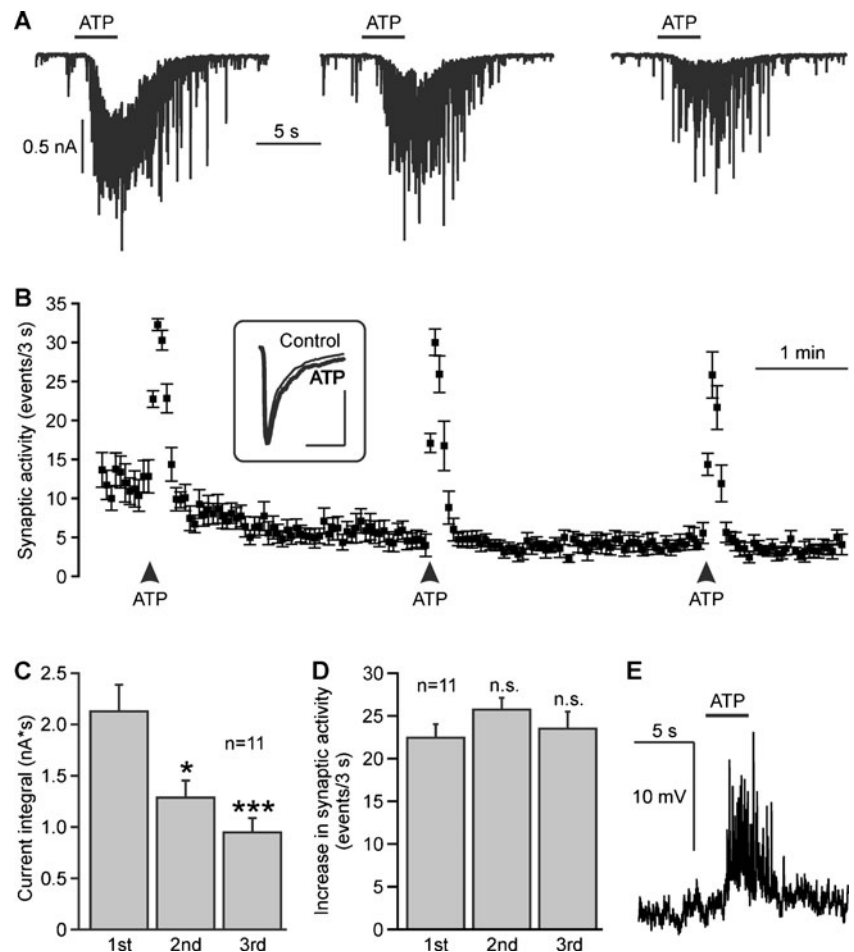
Photolysis of caged ATP induces synaptic activity in mitral cells

Mitral cells were identified by their size and their location in the mitral cell layer (Supplementary figure 2) as well as by visualizing the morphology of the cell filled with Alexa 594 hydrazide via the patch pipette after the experiment (not shown). Whole-cell currents were recorded in mitral cells at a holding potential of -70 mV. The perfusion system was stopped and caged ATP was added to the bath, resulting in a final concentration of 100 μM caged ATP. The shutter of a UV lamp was opened for 3 s to cleave caged ATP and produce free ATP. UV illumination evoked a slow inward current, superimposed by bursts of synaptic events (Fig. 1a). Three repetitive UV illuminations at an interval of 3 min elicited bursts of synaptic events each time (Fig. 1b) and inward currents of decreasing size as measured by the integral of the current trace (Fig. 1c). On average, the current trace integral amounted to 2.1 ± 0.3 nA*s at the first photorelease of ATP, and significantly decreased to 1.3 ± 0.2 nA*s at the second, and 0.9 ± 0.1 nA*s at the third photorelease of ATP ($n=11$). The frequency of synaptic events increased by 22.1 ± 1.5 events/3 s upon a first photorelease of ATP, and increased by 25.4 ± 1.4 and 23.5 ± 2.0 events/3 s upon a second and third photorelease of ATP, respectively ($n=11$). Differences in the ATP-evoked increases of the frequency of synaptic events were not statistically significant. We also calculated the averaged amplitude of synaptic events before and during photolysis of caged ATP. The amplitude of synaptic events was 111.7 ± 14.5 pA before and 120.7 ± 117.8 pA during photorelease of ATP, the difference not being statistically significant ($n=11$; inset in Fig. 1b). As a control, we illuminated olfactory bulb slices with UV light in the absence of caged ATP, which failed to induce an increase in synaptic events or an inward current ($n=5$; not shown). In current clamp mode, photorelease of ATP was able to induce a depolarisation of 12.9 ± 1.2 mV ($n=4$) and postsynaptic potentials (Fig. 1e).

P2Y₁ receptors mediate bursts of synaptic activity

To identify the receptors responsible for the increase in synaptic activity upon photorelease of ATP, we used caged ADP instead of caged ATP. ADP is able to activate some of the P2Y receptors, but not P2X receptors. Photorelease (3 s) of ADP resulted in a burst of synaptic events, accompanied by slow inward currents with an integral of 3.2 ± 0.7 nA*s at the first UV illumination, 2.0 ± 0.6 nA*s at the second, and 1.3 ± 0.4 nA*s at the third UV illumination ($n=7$; Fig. 2a, b). In general, ADP evoked larger currents than ATP, however,

Fig. 1 Photolysis of caged ATP (NPE-ATP) evokes synaptic currents in mitral cells. **a** Repetitive application of ATP by photolysis of NPE-ATP (100 μ M) evokes inward currents with decreasing amplitudes. **b** Photorelease of ATP increases the frequency of postsynaptic currents. *Inset*: The averaged current of fast synaptic events before application of ATP (Control, *thin line*) is not significantly altered during application of ATP (*bold line*). Scale bars: 50 ms; 50 pA. **c** The ATP-induced inward currents, as measured as the integral of the current trace, decreased upon the second and third photolysis of caged ATP compared to the first photolysis. *, $p < 0.05$; ***, $p < 0.005$. **d** The ATP-elicited increase in the frequency of postsynaptic currents remained constant at all three photolysis of ATP. ns, not significant. **e** In current clamp mode, photolysis of caged ATP results in a membrane depolarisation



the differences in current trace integral evoked by ATP and ADP were not statistically significant.

We also studied the effects of the nonspecific P2 receptor antagonist PPADS (100 μ M) and 50 μ M of the competitive antagonist MRS 2179, a concentration used to specifically inhibit P2Y₁ receptors in tissue preparations [23, 24], on ATP-evoked currents in mitral cells. Wash-in of PPADS ($n=4$) and MRS 2179 ($n=10$) did not alter the steady-state frequency of spontaneous synaptic events, suggesting that there is no major tonic activation of P2 purinoceptors (not shown). In the presence of PPADS, the inward current at the first photorelease of ATP was reduced by 72.2% to 0.6 ± 0.3 nA*s, and by 89.8% to 0.2 ± 0.1 nA*s at the second photorelease of ATP compared to the control (100%; $n=4$; Fig. 2c). Likewise, MRS 2179 reduced the current by 61.2% to 0.8 ± 0.3 nA*s and by 81.9% to 0.2 ± 0.1 nA*s, respectively ($n=10$; Fig. 2d). In the presence of PPADS and MRS 2179, the ATP-induced inward current was significantly smaller as compared to the control (Fig. 2e), indicating that P2Y₁ receptors mainly mediate the increase in synaptic activity upon ATP photorelease.

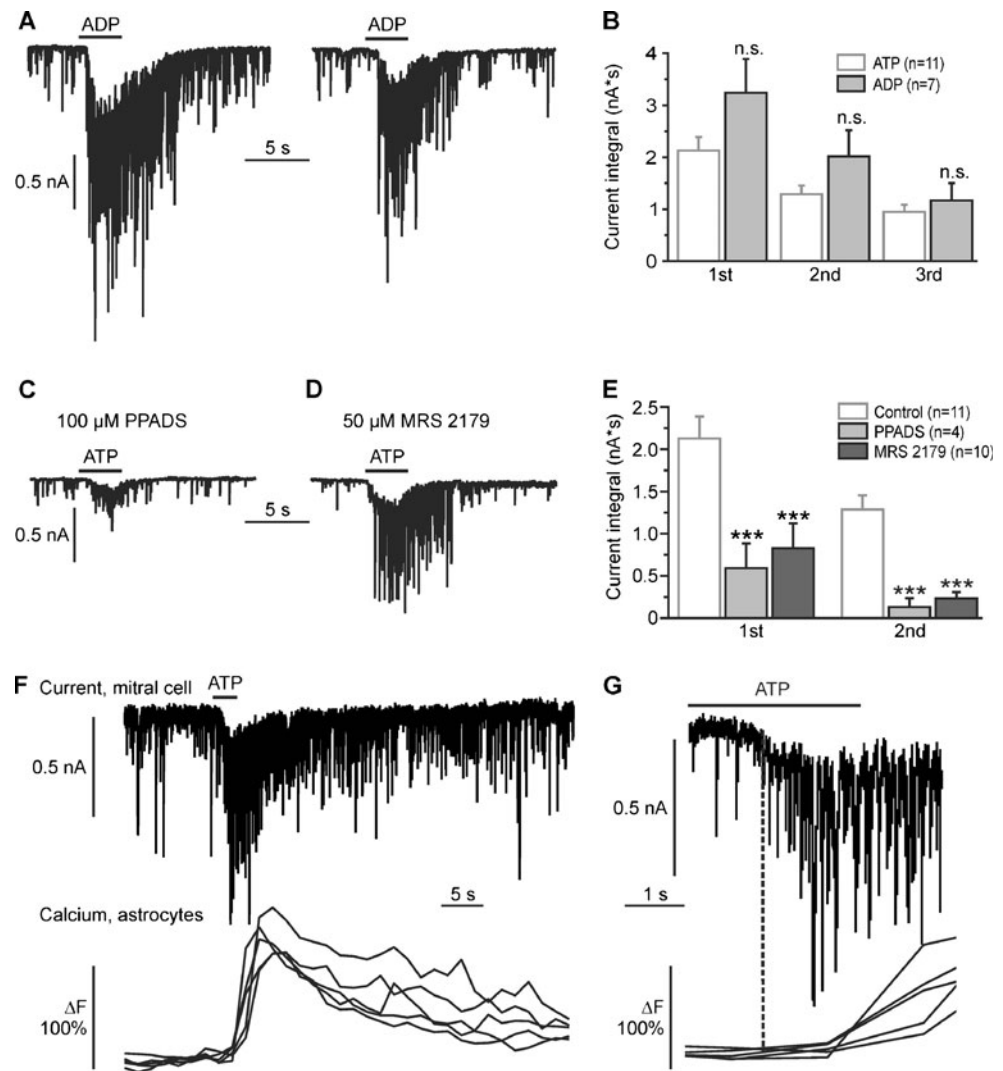
In the olfactory bulb, P2Y₁ receptors have been shown to trigger calcium signaling in astrocytes [16]. To test whether P2Y₁-mediated calcium signaling in astrocytes is causal for

the ATP-evoked inward currents in mitral cells, we measured membrane currents in mitral cells and calcium signaling in Fluo-4-loaded astrocytes simultaneously. Photolysis of caged ATP evoked inward currents in mitral cells which were followed by calcium transients in astrocytes. The onset of the current preceded the onset of astrocytic calcium transients by 2.4 ± 0.5 s ($n=6$ mitral cells compared with 30 astrocytes), indicating that the current is unlikely a consequence of astrocyte activation (Fig. 2f, g).

ATP does not directly stimulate mitral cells

The fast synaptic activity monitored by the mitral cell upon ATP photorelease reflects the firing activity of presynaptic neurons such as external tufted cells, periglomerular interneurons and granule cells, whereas the large inward current upon photorelease of ATP might be due to a direct action of ATP on mitral cells or the summation of a large number of synaptic currents. To separate direct effects of ATP on mitral cells from indirect effects, we suppressed action potential firing with the sodium channel blocker TTX (1–2 μ M). In the presence of TTX, photorelease of ATP failed to evoke an increase in synaptic events as well as an inward current in

Fig. 2 P2Y₁ receptors mediate the ATP-evoked increase in synaptic input in mitral cells. **a** Repetitive photorelease of ADP by photolysis of NPE-ADP (100 μM) evokes inward currents in mitral cells. **b** The difference between ADP-evoked inward currents and ATP-evoked inward currents was statistically not significant (n.s.). **c** Effects of the P2 receptor antagonist PPADS and (**d**) the P2Y₁-specific antagonist MRS 2179 on ATP-evoked inward currents. **e** ATP-evoked currents were significantly reduced by PPADS and MRS 2179. **f** Membrane current in a mitral cell (*upper trace*) and calcium transients in Fluo-4-loaded astrocytes (*lower traces*, five individual cells are shown as examples) evoked by photolysis of caged ATP. **g** Traces as shown in F at expanded time scale. The current response in the mitral cell precedes the calcium responses in astrocytes



mitral cells (Fig. 3a), suggesting that under control conditions both the increase in synaptic activity as well as the slow inward current reflects an increase in firing of presynaptic neurons, but not a direct stimulation of the recorded mitral cell.

To check whether the ATP-induced synaptic activity is glutamatergic or GABAergic, we first blocked GABA_A receptors with gabazine (10 μM) to isolate glutamatergic postsynaptic currents (Fig. 3b). In the presence of gabazine, photorelease of ATP evoked a slow inward current, but no fast postsynaptic currents. The integral of the inward current was reduced by 59.4% to 0.9 ± 0.3 nA*s at the first ATP photorelease and by 56.0% to 0.6 ± 0.2 nA*s at the second ATP photorelease compared to control recordings in the absence of gabazine ($n=6$; Fig. 3d). In contrast, in the presence of the ionotropic glutamate receptor blockers NBQX (10 μM) and D-AP5 (50 μM), used to isolate GABAergic postsynaptic currents, ATP photorelease failed to elicit a slow inward current, and induced only very few synaptic events (Fig. 3c).

The integral of the inward current was almost entirely reduced, on average by 90.5% to 0.2 ± 0.1 nA*s and by 88.3% to 0.1 ± 0.03 nA*s ($n=9$), respectively, at the first and second ATP photorelease (Fig. 3c, d). The results suggest that ATP primarily stimulates glutamatergic neurons which then drive the neuronal network in the olfactory bulb, including GABAergic neurons.

ATP-induced calcium signaling in the dendritic tuft of the mitral cell

Dendrites of mitral cells are highly compartmentalized, with a single central dendritic tuft projecting into a glomerulus where it receives glutamatergic input from olfactory sensory axons and tufted cells [25] as well as GABAergic input from interneurons, and several lateral dendrites which receive inhibitory input from GABAergic granule cells. To test the contribution of synaptic signaling in the dendritic tuft to the ATP-evoked responses in mitral cells, we simultaneously

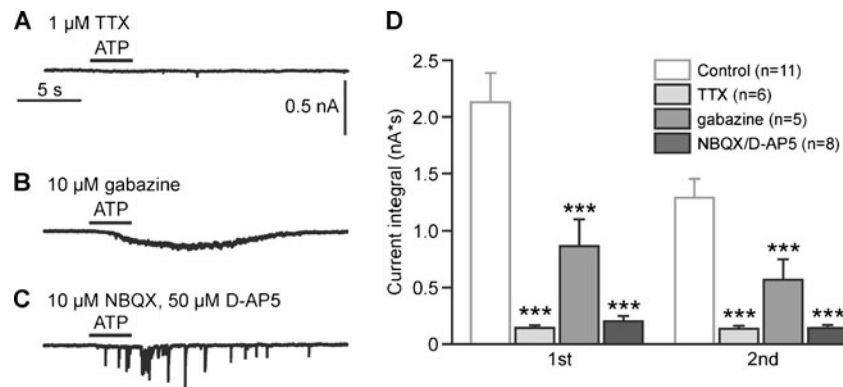


Fig. 3 The increase in synaptic input in mitral cells evoked by photolysis of caged ATP includes glutamatergic and GABAergic postsynaptic currents. **a** Effect of suppressing action potentials with TTX on ATP-evoked synaptic activity measured in a mitral cell. **b** Effect of inhibition of GABAergic transmission by gabazine, and **c** inhibition of glutamatergic transmission by NBQX/D-AP5 on ATP-induced synaptic input in mitral

cells. **d** Statistical evaluation of the effects of TTX (1–2 μM), gabazine (10 μM), and combined application of 10 μM NBQX and 50 μM D-AP5 on synaptic currents evoked by the first and second photolysis of caged ATP. All three drugs significantly reduced the current integral as compared to the control current recorded in the absence of antagonists. ***, $p < 0.005$

recorded calcium signaling in the dendritic tuft and synaptic whole-cell currents (Fig. 4a, b). Wide-field UV illumination (3 s) resulted in inward currents of 2.4 ± 0.3 nA*s ($n=9$) that were accompanied by an increase in calcium by 71.4 ± 18.9 ΔF ($n=4$). To test whether local photolysis of caged ATP in the glomerulus is sufficient to evoke responses in mitral cells, we illuminated a region of approximately 30×30 μm inside the glomerulus with a 405-nm laser (inset in Fig. 4c). Laser illumination resulted in an inward current of 1.1 ± 0.1 nA*s ($n=6$), but induced an increase in calcium in only one out of six experiments (Fig. 4c). The inward current evoked by local laser photolysis was significantly smaller than the inward current evoked by wide field photolysis ($p < 0.05$). The results demonstrate that P2Y₁ receptor activation in the glomerulus is sufficient to stimulate network activity, but often is not large enough to elicit measurable calcium signaling in the dendritic tuft under our experimental conditions.

Discussion

In the present paper, we studied the effect of ATP on neuronal network activity in the mouse olfactory bulb as monitored by synaptic events in mitral cells. The results demonstrate an increase in synaptic currents in mitral cells upon ATP photorelease, reflecting an increase in firing frequency in presynaptic neurons. This effect could be mimicked by the P2Y receptor ligand ADP and was largely inhibited by the P2Y₁ receptor antagonist MRS 2179, indicating that the increase in network activity is mainly mediated by P2Y₁ receptors. Hence, this study is the first to show that purinergic signaling affects neurons in the olfactory bulb.

P2 receptors in the olfactory bulb

The expression of different types of P2 receptors suggest a prominent role of purinergic signaling in the mammalian

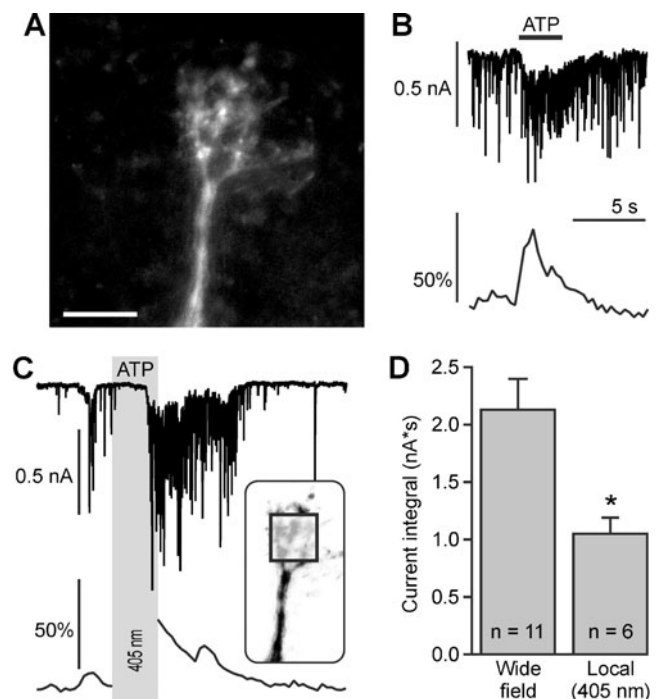


Fig. 4 Photolysis of caged ATP evokes calcium signaling in the dendritic tuft of mitral cells. **a** Confocal image of a Fluo-8-filled dendritic tuft. Scale bar, 30 μm. **b** Synaptic currents (upper trace) and calcium signaling (lower trace) elicited by wide-field photolysis of NPE-ATP (100 μM). **c** Synaptic currents (upper trace) and calcium signaling (lower trace) elicited by local photolysis of NPE-ATP (100 μM). The calcium imaging was interrupted during the time of ATP photolysis (gray bar). The square in the inset, depicting the dendritic tuft, indicates the area where the 405-nm laser was directed to. **d** Local photolysis of caged ATP evoked significantly smaller currents compared to wide-field photolysis. *, $p < 0.05$

olfactory bulb, emphasized by the high abundance of ectonucleotidases [26]. P2X₂ RNA was detected in olfactory bulb tissue using in situ hybridisation [27], and mitral cells, tufted cells as well as granule cells were stained with anti-P2X₂ antibodies [18, 20]. P2X₄ RNA and protein was also demonstrated in the olfactory bulb, with particular high expression in mitral cells [19, 28–31]. In addition, P2X₅ and P2X₆ expression was detected in mitral cells [17, 28]. An effect of ATP on cells in the olfactory bulb has been shown in *Xenopus* tadpoles, where calcium signaling is mediated by P2X receptors [32], however, in that study the cell type sensitive to ATP could not be identified. Despite the abundant expression of P2X receptors in the olfactory bulb, we could not record ionic currents attributable to P2X receptor activation in mitral cells. We used photolysis of caged ATP, which results in a rapid rise in extracellular ATP. Hence, P2X receptor desensitization appears not to be a likely explanation for the lack of P2X-mediated currents. The concentration of caged ATP applied to the brain slices was 100 μM and 100 μM of free ATP is sufficient to saturate the current response of heterologously expressed P2X receptors [27–31]. However, we have no measure of the efficacy of photolysis of caged ATP or the enzymatic cleavage of ATP, and thus cannot estimate the actual concentration of free ATP in the tissue after photolysis. The concentration of free ATP might have been too low for efficient P2X receptor activation, but was sufficient to stimulate P2Y₁ receptors which are about one order of potency more sensitive than some of the P2X receptors [16, 33]. P2Y₁ receptors are widely expressed in the olfactory bulb, including the glomerular layer, external plexiform layer, granule cell layer, and nerve layer [34]. Functional expression has so far only been demonstrated in glial cells of the olfactory bulb. Activation of P2Y₁ receptors in olfactory bulb astrocytes results in calcium transients, whereas vesicular ATP release from olfactory axons in the nerve layer stimulates P2Y₁ receptor-mediated calcium signaling in adjacent ensheathing glial cells and thereby mediates neurovascular coupling [15, 16]. Here, we present evidence that P2Y₁ receptors can also stimulate neurons in the olfactory bulb.

Mechanism of ATP-mediated stimulation of network activity

The present study demonstrates that P2Y₁ receptor activation not only acts on olfactory bulb glial cells, but also affects neuronal performance and elicits inward currents and calcium signaling in mitral cells. Since the effect was blocked in the presence of TTX, P2Y₁ receptors are most likely not activated in the mitral cells themselves, but in presynaptic neurons such as interneurons and tufted cells. The primary target cells of ATP appear to be glutamatergic, since blocking glutamate receptors almost entirely suppressed the P2Y₁ receptor-mediated enhancement of network activity. External tufted

cells are glutamatergic and drive the network activity in glomeruli in the olfactory bulb [21, 25] and therefore are likely candidates for ATP targets. The dendrites of external tufted cells project into a glomerulus and local photolysis of ATP in a single glomerulus was sufficient to stimulate network activity. However, this was not accompanied by dendritic calcium signaling in the majority of the experiments using local photolysis. Since the current response evoked by local photolysis was much smaller than the one induced by wide-field illumination, the increase in neuronal activity probably was not large enough to evoke measurable calcium transients in the mitral cell dendrite. Olfactory bulb astrocytes express P2Y₁ receptors and modulate neuronal excitability as well as synaptic transmission in the olfactory bulb [16, 35], suggesting the possibility that the increase in neuronal activity upon photo-release of ATP is a consequence of ATP-mediated activation of astrocytes. However, Kozlov et al. [35] described a GABAergic inhibitory effect of astrocytes on mitral cells, in contrast to the glutamatergic excitatory effect shown here. In addition, TTX, which does not affect astrocyte performance, strongly suppressed the P2Y₁ receptor-mediated enhancement of network activity, rendering astrocytes as less likely candidates for the ATP-dependent effect measured in the present study. This is confirmed by the delay of ATP-induced astrocytic calcium signaling with respect to the recorded inward current in mitral cells.

Conclusion

Our study provides first evidence that ATP, recently described as neurotransmitter acting on glial cells in the olfactory bulb, also affects neuronal performance in this brain region. ATP stimulates P2Y₁ receptors and thereby increases neuronal network activity, leading to depolarisation and calcium transients in dendritic tufts of mitral cells.

Acknowledgments Supported by the Deutsche Forschungsgemeinschaft (LO 779/6).

References

1. Burnstock G (2006) Pathophysiology and therapeutic potential of purinergic signaling. *Pharmacol Rev* 58:58–86
2. Burnstock G (2007) Physiology and pathophysiology of purinergic neurotransmission. *Physiol Rev* 87:659–797
3. Abbracchio M, Burnstock G, Verkhratsky A, Zimmermann H (2009) Purinergic signalling in the nervous system: an overview. *Trends Neurosci* 32:19–29
4. Illes P, Alexandre Ribeiro J (2004) Molecular physiology of P2 receptors in the central nervous system. *Eur J Pharmacol* 483:5–17
5. Zimmermann H (2009) Ectonucleotidases in the nervous system. *Novartis Found Symp* 276:113–128, discussion 128–30, 233–7, 275–81
6. Burnstock G, Fredholm B, Verkhratsky A (2011) Adenosine and ATP receptors in the brain. *Curr Top Med Chem* 11:973–1011

7. Edwards FA, Gibb AJ, Colquhoun D (1992) ATP receptor-mediated synaptic currents in the central nervous system. *Nature* 359:144–147
8. Pankratov Y, Castro E, Miras-Portugal MT, Krishtal O (1998) A purinergic component of the excitatory postsynaptic current mediated by P2X receptors in the CA1 neurons of the rat hippocampus. *Eur J Neurosci* 10:3898–3902
9. Pankratov Y, Lalo U, Verkhratsky A, North R (2007) Quantal release of ATP in mouse cortex. *J Gen Physiol* 129:257–265
10. Goncalves J, Queiroz G (2008) Presynaptic adenosine and P2Y receptors. *Handb Exp Pharmacol* 184:339–372
11. Deitmer JW, Brockhaus J, Casel D (2006) Modulation of synaptic activity in Purkinje neurons by ATP. *Cerebellum* 5:49–54
12. Bilbao PS, Katz S, Boland R (2011) Interaction of purinergic receptors with GPCRs, ion channels, tyrosine kinase and steroid hormone receptors orchestrates cell function. *Purinergic Signal*. doi:10.1007/s11302-011-9260-9
13. Lohr C, Thyssen A, Himet D (2011) Extrasynaptic neuron-glia communication: the how and why. *Commun Integr Biol* 4:109–111
14. Rieger A, Deitmer JW, Lohr C (2007) Axon-glia communication evokes calcium signaling in olfactory ensheathing cells of the developing olfactory bulb. *Glia* 55:352–359
15. Thyssen A, Hirnet D, Wolburg H, Schmalzing G, Deitmer J, Lohr C (2010) Ectopic vesicular neurotransmitter release along sensory axons mediates neurovascular coupling via glial calcium signaling. *Proc Natl Acad Sci U S A* 107:15258–15263
16. Doengi M, Deitmer J, Lohr C (2008) New evidence for purinergic signaling in the olfactory bulb: A2A and P2Y1 receptors mediate intracellular calcium release in astrocytes. *FASEB J* 22:2368–2378
17. Guo W, Xu X, Gao X, Burnstock G, He C, Xiang Z (2008) Expression of P2X5 receptors in the mouse CNS. *Neuroscience* 156:673–692
18. Kanjhan R, Housley GD, Burton LD, Christie DL, Kippenberger A, Thorne PR, Luo L, Ryan AF (1999) Distribution of the P2X2 receptor subunit of the ATP-gated ion channels in the rat central nervous system. *J Comp Neurol* 407:11–32
19. Le KT, Villeneuve P, Ramjaun AR, McPherson PS, Beaudet A, Seguela P (1998) Sensory presynaptic and widespread somatodendritic immunolocalization of central ionotropic P2X ATP receptors. *Neuroscience* 83:177–190
20. Vulchanova L, Arvidsson U, Riedl M, Wang J, Buell G, Surprenant A, North RA, Elde R (1996) Differential distribution of two ATP-gated channels (P2X receptors) determined by immunocytochemistry. *Proc Natl Acad Sci U S A* 93:8063–8067
21. De Saint JD, Himet D, Westbrook G, Charpak S (2009) External tufted cells drive the output of olfactory bulb glomeruli. *J Neurosci* 29:2043–2052
22. Doengi M, Coulon P, Pape HC, Deitmer JW, Lohr C (2009) GABA uptake-dependent Ca²⁺ signaling in developing olfactory bulb astrocytes. *Proc Natl Acad Sci U S A* 106:17570–17575
23. Wurm A, Lipp S, Pannicke T, Linnertz R, Krügel U, Schulz A, Färber K, Zahn D, Grosse J, Wiedemann P, Chen J, Schöneberg T, Illes P, Reichenbach A, Bringmann A (2010) Endogenous purinergic signaling is required for osmotic volume regulation of retinal glial cells. *J Neurochem* 112:1261–1272
24. Hamilton N, Vayro S, Wigley R, Butt AM (2010) Axons and astrocytes release ATP and glutamate to evoke calcium signals in NG2-glia. *Glia* 58:66–79
25. Najac M, De Saint JD, Reguero L, Grandes P, Charpak S (2011) Monosynaptic and polysynaptic feed-forward inputs to mitral cells from olfactory sensory neurons. *J Neurosci* 31:8722–8729
26. Langer D, Hammer K, Koszalka P, Schrader J, Robson S, Zimmermann H (2008) Distribution of ectonucleotidases in the rodent brain revisited. *Cell Tissue Res* 334:199–217
27. Simon J, Kidd EJ, Smith FM, Chessell IP, Murrell-Lagnado R, Humphrey PP, Barnard EA (1997) Localization and functional expression of splice variants of the P2X2 receptor. *Mol Pharmacol* 52:237–248
28. Collo G, North RA, Kawashima E, Merlo-Pich E, Neidhart S, Surprenant A, Buell G (1996) Cloning OF P2X5 and P2X6 receptors and the distribution and properties of an extended family of ATP-gated ion channels. *J Neurosci* 16:2495–2507
29. Soto F, Garcia-Guzman M, Gomez-Hernandez JM, Hollmann M, Karschin C, Stuhmer W (1996) P2X4: an ATP-activated ionotropic receptor cloned from rat brain. *Proc Natl Acad Sci U S A* 93:3684–3688
30. Buell G, Lewis C, Collo G, North RA, Surprenant A (1996) An antagonist-insensitive P2X receptor expressed in epithelia and brain. *EMBO J* 15:55–62
31. Bo X, Zhang Y, Nassar M, Burnstock G, Schoepfer R (1995) A P2X purinoceptor cDNA conferring a novel pharmacological profile. *FEBS Lett* 375:129–133
32. Hassenklöver T, Schulz P, Peters A, Schwartz P, Schild D, Manzini I (2010) Purinergic receptor-mediated Ca signaling in the olfactory bulb and the neurogenic area of the lateral ventricles. *Purinergic Signal* 6:429–445
33. Schachter JB, Li Q, Boyer JL, Nicholas RA, Harden TK (1996) Second messenger cascade specificity and pharmacological selectivity of the human P2Y1-purinoceptor. *Br J Pharmacol* 118:167–173
34. Simon J, Webb TE, Barnard EA (1997) Distribution of dATP alpha S binding sites in the adult rat neuraxis. *Neuropharmacology* 36:1243–1251
35. Kozlov AS, Angulo MC, Audinat E, Charpak S (2006) Target cell-specific modulation of neuronal activity by astrocytes. *Proc Natl Acad Sci U S A* 103:10058–10063